Chemorheology of an Epoxy Resin System under Isothermal Curing

T. H. HOU, *Structures and Materials Department, Lockheed Engineering and Sciences Company, Hampton, Virginia 23666,* and JOAN Y. Z. HUANG* and J. A. HINKLEY,† *NASA Langley Research Center, MS 226, Hampton, Virginia 23665-5225*

Synopsis

The chemorheological properties of a commercial Hercules 3501-6 resin system were studied under isothermal curing conditions between 375 and 435 K. For cure temperatures ≥ 385 K, the storage modulus curing curves, $G'(t)$, exhibited abrupt changes in slope which occurred at various times depending on the curing temperatures. These slope changes were attributed to the onset of gelation. Crossover points between $G'(t)$ and $G''(t)$ curves were observed for curing temperatures ≥ 400 K. The gelation and the crossover points obtained from the chemorheological measurements, therefore, defined two characteristic resin states during cure. Although gelation theory did not predict them correctly, the degree of cure in each of these states was approximately the same for every cure temperature. The temperature dependency of the viscosities in the characteristic resin states, and the rate constants of increase in moduli at different stages of curing were analyzed. Various $G'(t)$ and $G''(t)$ isothermal curing curves were also shown to be capable of being superimposed to one another by the principle of time-temperature superposition. The resultant shift factors $a_t(T)$ and $a_\eta(T)$ were shown to follow Arrhenius type relationships. Values of the activation energy suggested that the reaction kinetics, instead of the diffusion mechanism, was the limiting step in the overall resin advancement for cure at temperatures ≥ 385 K.

INTRODUCTION

Rheology is a science that deals with the deformation and flow of material under stress. Understanding the rheological properties of polymeric materials has played an increasingly critical role for the successful processing of such materials. For a given thermoplastic melt, the viscoelastic properties are determined by processing temperatures and flow geometry. In the processing of a thermosetting resin, chemorheology is influenced by one additional factor, i.e., the reaction kinetics of the resin system. Processing temperature affects the chemoviscosity rise profile in two opposing ways. An increase in temperature lowers the chemoviscosity at a given extent of reaction, but also increases the reaction rate, which eventually leads to an increase in the resin viscosity. It is therefore essential to obtain chemorheology data as a function of reaction kinetics and temperature for the purposes of material characterization and process modeling. Unlike the results of more conventional characterization techniques, such as stoichiometry, calorimetry and spectrometry, the rheological measure-

* Present address: Department of Mechanical Engineering and Mechanics, Old Dominion University, Norfolk, Virginia 23508.

† To whom correspondence should be addressed.

Journal of Applied Polymer Science, Vol. 41, 819–834 (1990)
 CCC 0021-8995/90/3-40819-16$04.00

ments are directly useful to the processing engineer who is concerned with the behavior of resin flow.[1-4] It is well known that viscoelastic properties are sensitive to the macromolecular chain length and branching. During the cure of thermosetting resins, the structure of the resin polymer undergoes a continuous transformation from a low molecular weight liquid to a high molecular weight melt and eventually transforms to a crosslinked network. Changes in the slopes of curves defining viscoelastic properties versus reaction time should directly reflect such transformations within the material. By performing experiments at constant temperature, it is even possible to relate the viscoelastic property–time profiles to the reaction kinetics of the resin system under cure.

In this paper we report an experimental study of the changes in rheological properties of a thermosetting resin system cured under several isothermal conditions.

MATERIAL

As-received commercial Hercules 3501-6[‡] epoxy resin was used without further treatments in this study. This material was selected because of its wide usage in the aerospace industry. Concentrations of the starting components of the Hercules 3501-6 epoxy[5-7] are summarized in Table I.

Test samples were preconditioned at room temperature by pressing between two pieces of nonporous Teflon cloth to produce flat sheets with given uniform thickness. A resin wafer of 1.2 mm in thickness and 1.25 cm in diameter was then made with a steel guide. All samples were stored at −5°C before being loaded in the rheometer for rheological measurements.

EXPERIMENTAL

A Rheometrics System 4 rheometer fitted with a parallel-plate test cell was used for the rheological measurements. The test sample was confined in the gap between two parallel 1.25 cm radius plates. The top plate was oscillated at a given frequency and amplitude, while the bottom plate was mounted on a

[‡] Hercules 3501-6 resin is manufactured by the Hercules Aerospace Company, Magna, UT. Use of trade names or manufacturers does not constitute an official endorsement, either expressed or implied, by the National Aeronautics and Space Administration.

TABLE I
Typical Epoxy Formulation

Component	Wt %	Assumed functionality	Eq wt
Tetraglycidyl methylene dianiline (TGMDA)	56.5	4.0	105.5
Alicyclic diepoxy carboxylate	9.0	2.0	118.0
Epoxy cresol novolac	8.5	6.0	225.0
4,4'-Diaminodiphenyl sulfone (DDS)	25.0	4.0	62.0
Borontrifluoride amine complex	1.1	—	—

torque transducer for force measurements. The typical gap between the plates was 1.2 mm. The plates and test samples were enclosed in a heat chamber purged with nitrogen gas. The test chamber was always preheated to the test temperature before loading each sample to insure precise gap settings.

The amplitude of oscillation of the top plate was selected to assure that the strains imposed on the sample during measurement were within its linear viscoelastic response range while maintaining adequate torque values. Typical measurements on this particular resin system usually started at 0.5 strain level. Strain values were decreased stepwise down to about 0.001 during the cure cycle due to the increasing rigidity of the sample. Plate oscillatory motion was set at a frequency of $\omega = 10$ rad/s. Repeatability of the measurements performed at each cure temperature was always checked by selecting various strain values during the cure cycle. The recorded cyclic torque values were decomposed into in-phase and out-of-phase components with respect to the oscillatory deformation imposed on the sample. The corresponding storage (G') and loss (G'') moduli were obtained from these components. The complex viscosity η^* was then calculated directly from $\eta^* = (G'^2 + G''^2)^{1/2}/\omega$.

RESULTS AND DISCUSSION

Rheological measurements were made isothermally on the Hercules 3501-6 resin system at six selected temperatures between 375 and 435 K. Typical double logarithmic plots for the storage, $G'(t)$, and loss, $G''(t)$, moduli as functions of reaction time t at 375, 385, 400, and 425 K are shown in Figures 1–4, respectively. Moduli measurements ranged from 10 to 10^7 dyn/cm^2. Measured values above 10^7 dyn/cm^2 are not reported in the figures, due to the possibility of slippage between the rigid sample and the rheometer tool plates during the latter stages of curing. The loss moduli were observed to increase smoothly over the entire cure cycle. In contrast, however, the storage moduli $G'(t)$ ex-

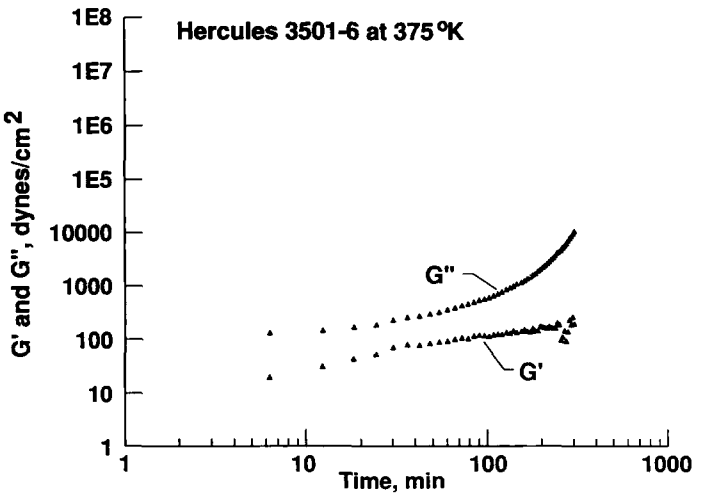

Fig. 1. Storage modulus G' and loss modulus G'' as functions of time for Hercules 3501-6 resin cured at 375 K.

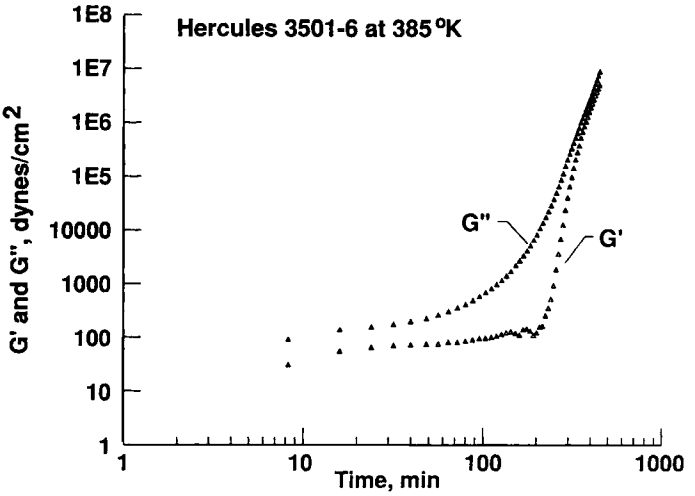

Fig. 2. Storage modulus G' and loss modulus G'' as functions of time for Hercules 3501-6 resin cured at 385 K.

hibited abrupt changes in slope at different curing times for samples cured at temperatures above 375 K. At higher cure temperatures, the abrupt changes in slope occurred earlier in the cure cycle.

Another characteristic of the curing behavior of Hercules 3501-6 epoxy is that the $G'(t)$ and $G''(t)$ curves cross at certain curing times at temperatures above 385 K. The G' and G'' coincide over a period of time during cure at 400 K, and a single crossover point is observed when higher curing temperatures are employed. Some properties associated with these curing characteristics are summarized in Tables II and III. The subscript o refers to the onset of the

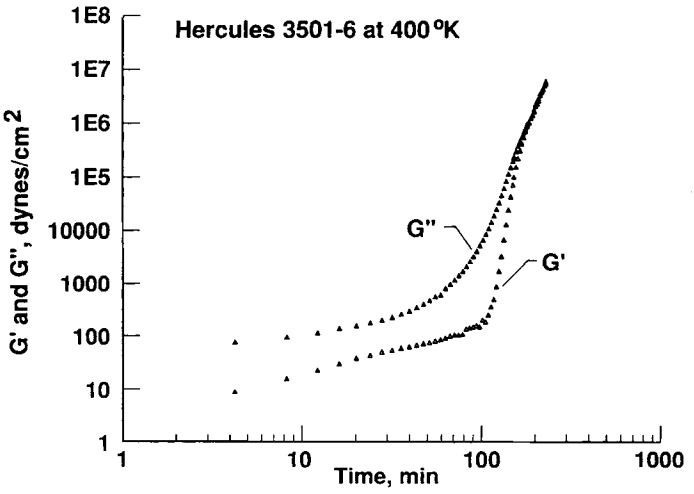

Fig. 3. Storage modulus G' and loss modulus G'' as functions of time for Hercules 3501-6 resin cured at 400 K.

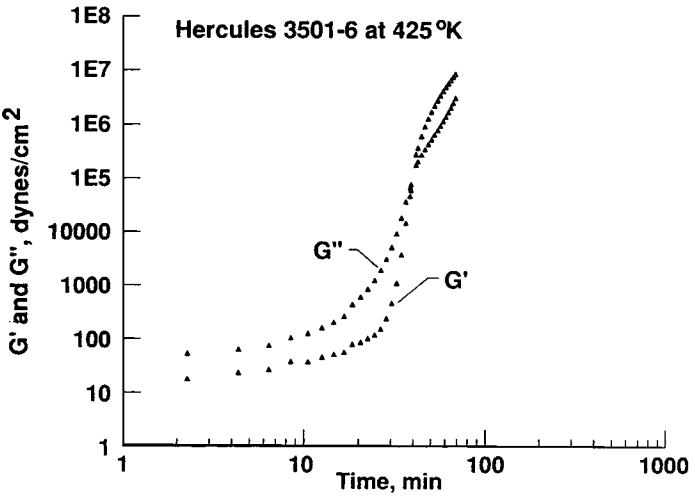

Fig. 4. Storage modulus G' and loss modulus G'' as functions of time for Hercules 3501-6 resin cured at 425 K.

abrupt change in $G'(t)$, and the subscript c denotes the crossover point between the $G'(t)$ and $G''(t)$ curves.

Lee et al.[8] reported DSC thermal analysis data on the same resin system cured under isothermal conditions. The degree of cure $\alpha(t)$ was equated to the fraction of the total heat of reaction released up to the time t. The following equations were found to describe the degree of cure α rather satisfactorily:

$$\frac{d\alpha}{dt} = (K_1 + K_2\alpha)(1 - \alpha)(B - \alpha) \qquad \text{for } \alpha < 0.3 \tag{1a}$$

$$\frac{d\alpha}{dt} = K_3(1 - \alpha) \qquad \text{for } \alpha > 0.3 \tag{1b}$$

where $K_1 = A_1 \exp(-\Delta E_1/RT)$, $K_2 = A_2 \exp(-\Delta E_2/RT)$, $K_3 = A_3 \exp(-\Delta E_3/RT)$. Values of the constants are summarized in Table IV. Values of α_o and α_c calculated from Eqs. (1a, b) are also included in Tables II and III for samples cured at various specified isothermal conditions.

TABLE II
Properties Associated with the Onset of Abrupt Change in Storage Moduli $G'(t)$ during the Isothermal Curing of Hercules 3501-6 Resin System

T (K)	t_o (min)	G'_o (10^2 dyn/cm^2)	G''_o (10^3 dyn/cm^2)	η^*_o (10^2 P)	α_o
375	—	—	—	—	—
385	220	1.8	15.0	15.0	0.57
400	110	2.3	7.0	7.0	0.59
410	65	1.6	5.4	5.4	0.59
425	25	1.2	2.1	2.1	0.52
435	12	0.84	1.6	1.6	0.45

TABLE III
Properties Associated with the Crossover Point between $G'(t)$ and $G''(t)$ during the Isothermal Curing of Hercules 3501-6 Resin System

T (K)	t_c (min)	$G'_c = G''_c$ (10^4 dyn/cm^2)	η_c^* (10^4 P)	α_c
375	—	—	—	—
385	—	—	—	—
400	182	71.0	10.0	0.76
410	95	28.0	4.0	0.72
425	39	10.0	1.4	0.64
435	19	4.7	0.67	0.55

Gelation Point

The gel point of a crosslinking polymer refers to the appearance of gel by the advancement of reactions during cure. At the molecular level, a gel is formed when at least one of the molecules has grown very large and its size reaches dimensions on the order of the macroscopic sample.[9] The gel point may be determined by measuring various resin properties. In the steady state shear experiment, for example, the gel point is commonly defined as the time when shear viscosity becomes infinite, or when the equilibrium modulus becomes nontrivial.[2–4] In practice, however, the gel point is determined at the point when the steady shear viscosity reaches 10^3 P and the resin ceases to flow readily. In the dynamic experiment, the gel point has sometimes been located by the crossover point between the $G'(t)$ and $G''(t)$ curves.[10] Recently, Winter et al. have suggested a constitutive equation for network polymers at the gel point.[11,12] The constitutive equation shows that the crossover points where $G'(\omega) = G''(\omega)$ are indeed a rheological property at the gel point for the polydimethylsiloxane (PDMS) polymer used in their experiments.[11]

From the experimentally measured $G'(t)$ and $G''(t)$ for the Hercules 3501-6 resin system cured at different isothermal conditions, we noted that, at temperatures below 385 K (375 K cure, for example), neither an abrupt change in slope of the $G'(t)$ curve nor a crossover point was observed (see Fig. 1), and the resin did not gel at any point in the entire cure cycle. At 385 K, a distinct change in slope of the $G'(t)$ curve was observed. Since storage modulus G' is a measure of resin elasticity, a dramatic increase in $G'(t)$ indicates the initiation of a gel network. However, $G'(t)$ is consistently lower than $G''(t)$ over the

TABLE IV
Values of Constants in Eqs. (1a), and (1b) for Hercules 3501-6 Resin System

$B = 0.47$
$A_1 = 2.101 \times 10^9$ min^{-1}
$A_2 = 2.014 \times 10^9$ min^{-1}
$A_3 = 1.960 \times 10^5$ min^{-1}
$\Delta E_1 = 8.07 \times 10^4$ J/mol
$\Delta E_2 = 7.78 \times 10^4$ J/mol
$\Delta E_3 = 5.66 \times 10^4$ J/mol

entire cure cycle. The largest G'/G'' equals 0.625 and occurs at about $t = 400$ min (see Fig. 2). For $T \geq 400$ K, each curing curve possesses not only a distinct change in slope of the $G'(t)$ curve but also a crossover point between $G'(t)$ and $G''(t)$. Consequently, it seems more appropriate to assign the gel point for the resin system studied here to the onset of the abrupt change in slope of the $G'(t)$ curing curves under these various isothermal curing conditions. It is noted that, at the assigned gel points, G' is lower than G'' by almost 2 orders of magnitude, and the resin is basically liquidlike. The incipient crosslinked network has zero stiffness at the gel point, but its contribution increases rapidly thereafter.

It is conceivable that both the gelation point and the crossover point for resin samples cured at various temperatures higher than 385 K, define uniquely two common material states during the advancement of reactions. The nearly constant values of the observed α_o in Table II seems to support such a speculation. Values of α_c in Table III show larger scatters, which could be attributed to the extrapolation errors introduced by extending eqs. (1) outside the range of α originally covered by the study of Lee et al.[8] If the speculation is correct, then variations of the complex viscosities η_o^* and η_c^* in Tables II and III are solely due to temperature effects.

Temperature Dependent Viscosities

In numerous studies of polymeric liquids, the complex viscosities $\eta^*(\omega)$ have been observed to closely resemble $\eta(\dot{\gamma})$, where $\eta(\dot{\gamma})$ is the steady shear viscosity at shear rate $\dot{\gamma}$. This relationship $\eta(\dot{\gamma}) = \eta^*(\omega)$ is known as the Cox–Merz rule.[13] This rule has proven to be very useful in predicting $\eta(\dot{\gamma})$ when only linear viscoelastic data are available.[14] Consequently, the temperature dependent behaviors of viscosities η_o^* and η_c^* are investigated according to the following formula:

$$-(T - T_r)/\log a_T = (T - T_r)/C_1 + C_2/C_1 \tag{2}$$

$$\eta^* = A \exp(E_\eta/RT) \tag{3}$$

Equation (2) is derived from the Williams–Landel–Ferry (WLF) equation with $a_T = \eta^*(T)/\eta^*(T_r)$.[15] C_1 and C_2 are material parameters, and $T_r = 400$ K was selected as the reference temperature. Equation (3) is the so-called Arrhenius type relationship, with $R = 1.986$ cal/mol/K, the ideal gas constant, and E_η, the activation energy for viscous flow. Equations (2) and (3) predict that the plot of $-(T - T_r)/\log a_T$ vs. $(T - T_r)$ or $\ln \eta^*$ vs. $(1/T)$ should be linear for temperature dependency following either the WLF type or the Arrhenius type, respectively.

Results of the linear least squares fit of Eqs. (2) and (3) to the experimental data (see Tables II and III) are tabulated in Table V. It is noted that $\eta^*(T)$ can be more accurately described by the Arrhenius type of temperature dependency in both characteristic resin states. Arrhenius behavior is usually observed above $T_g + 100$ K. This suggests that the glass transition temperature T_g of the material remains less than approximately $(T_d - 100)$ K up to the crossover point t_c, of $G'(t)$ and $G''(t)$ during the cure advancement at temperature T_d. Differential scanning calorimetry on the partially cured resin[16] confirms that this is the case at least up to $\alpha = 0.6$.

TABLE V
Linear Least Squares Results of Eqs. (2) and (3) for the Temperature Dependence of Viscosities

Resin state	Parameter[a]	WLF type [eq. (2)]	Arrhenius type [eq. (3)]
Gelation point	R_o	0.049	0.994
	P_o	58.43	7.70
	Q_o	0.045	12.71
Crossover point	R_c	0.952	0.999
	P_c	23.51	13.19
	Q_c	0.195	21.54

[a] Subscripts o and c refer to gelation point and crossover point respectively.

R_o, R_c denote correlation coefficients from least squares. $P = C_2/C_1$ (deg) and $Q = 1/C_1$ in eq. (2). $P = E_\eta/R$ (K) and $Q = \ln A$ (P) in eq. (3).

Overall Reaction Kinetics of Resin Advancement

It is also of interest to compare the activation energies for the polymerization reaction E_a and for viscous flow E_η at the two characteristic material states during cure. Assuming that the inverse of reaction time t has the same temperature dependency as the overall reaction rate constant k_p, then

$$t = 1/k_p = A_t \exp(E_a/RT) \tag{4}$$

A semilogarithmic plot of $\ln t$ vs. $(1/T)$ should yield the apparent activation energy of polymerization, E_a. Values of E_a, together with values of E_η obtained from eq. (3) and Table V are summarized in Table VI. Within the range of curing temperatures investigated here, the higher value of E_a compared to E_η at the gelation point clearly suggests that the chemical reaction is the limiting step for the rate of advancement of the resin system during cure. On the other hand, a higher value of E_η than E_a at the crossover point suggests that the limiting step for the resin advancement becomes diffusion controlled.

In the semilogarithmic plots of $G'(t)$ and $G''(t)$ shown in Figures 5 and 6, the slopes of the curves represent the reaction rate constants k, which dictate the rates of increase of the moduli. Also shown in the figures are arrow marks which identify the gelation and crossover points. For the curing temperatures $\geq$ 400 K, the crossover points become evident. It is noted that beyond the crossover points, both $G'(t)$ and $G''(t)$ curves are straight lines, which correspond to a first-order reaction. The slopes of these straight lines, k_{pc}, are tabulated in Table VII, which shows that values of $k_{pc,G'}$ are approximately equal

TABLE VI
Activation Energies of E_a and E_η at the Two Characteristic Material States during the Cure of Hercules 3501-6 Resin System

Material state	E_a (kcal/mol)	E_η (kcal/mol)
Gelation point	19.3	15.3
Crossover point	22.0	26.2

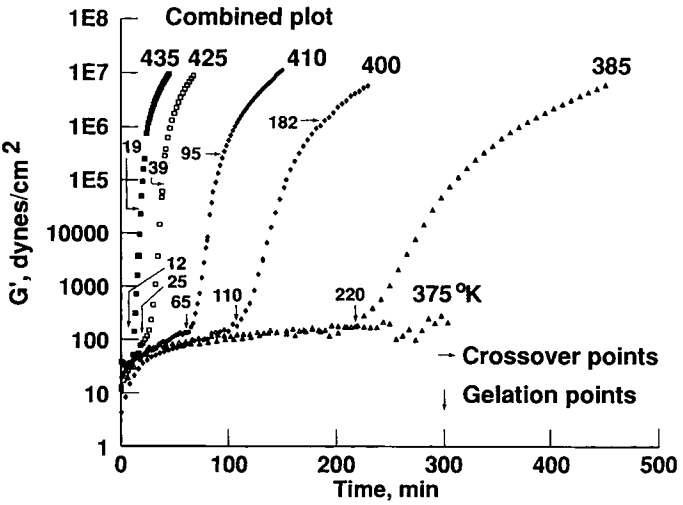

Fig. 5. Semilogarithmic plots of $G'(t)$ for Hercules 3501-6 resin cured under six isothermal curing temperatures. (the gelation and crossover points are marked by arrows).

to $k_{pc,G''}$, where the subscript pc denotes post crossover, and the subscripts G' and G'' refer to the $G'(t)$ and $G''(t)$ curves, respectively.

Not far away into the cure beyond the gelation points, the semilogarithmic plots of $G'(t)$ and $G''(t)$ are also characterized by straight lines as well. These straight lines span 2–3 orders of magnitude in moduli. The slopes k_{po}, where subscript po denotes post gelation, are also tabulated in Table VII. Ratios of $k_{po,G'}/k_{po,G''}$ are noted to vary between 2.00 and 2.33 under various isothermal curing temperatures.

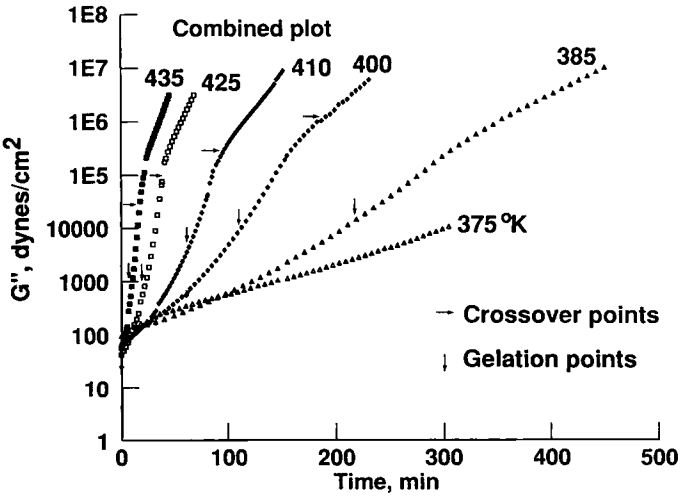

Fig. 6. Semilogarithmic plots of $G''(t)$ for Hercules 3501-6 resin cured under six isothermal curing temperatures. (the gelation and crossover points are marked by arrows).

TABLE VII
Rate Constants at Different Reaction Zones during the Isothermal Curing of Hercules 3501-6 Resin System

	$G'(t)$ curve		$G''(t)$ curve	
T (K)	k_{po} (min^{-1})	k_{pc} (min^{-1})	k_{po} (min^{-1})	k_{pc} (min^{-1})
375	—	—	—	—
385	0.035	—	0.015	—
400	0.072	0.018	0.033	0.017
410	0.14	0.020	0.068	0.024
425	0.27	0.034	0.120	0.040
435	0.48	0.051	0.241	0.053

For linear flexible polymers with sufficiently high molecular weight M_w, such that the entanglement effects become evident, it is known in polymer rheology that $\eta_0 \sim M_w^{3.4}$ and $N_1 \sim M_w^{7.0}$,[14] where η_0 is the zero shear viscosity and N_1 is the first normal stress difference. N_1 and η_0 are analogous to the storage $G'(\omega)$ and loss $G''(\omega)$ moduli, which also measure elastic and dissipation factors, respectively, for our lightly crosslinked polymer. From the relationships $\eta_0 \sim G''(\omega)$ and $N_1(\dot{\gamma}) \sim G'(\omega)$, we predict

$$\frac{k_{po,G'}}{k_{po,G''}} = \frac{d \log G'(t)/dt}{d \log G''(t)/dt} = 2.1 \tag{5}$$

It is noted that the value of the ratio calculated by eq. (5) compares very favorably to the experimentally observed values in Table VII.

Correspondence between Cure Temperature and Reaction Time

Double logarithmic plots of the curing curves for Hercules 3501-6 are shown in Figures 7 and 8. It was noted that the curing curves of either $G'(t)$ or $G''(t)$

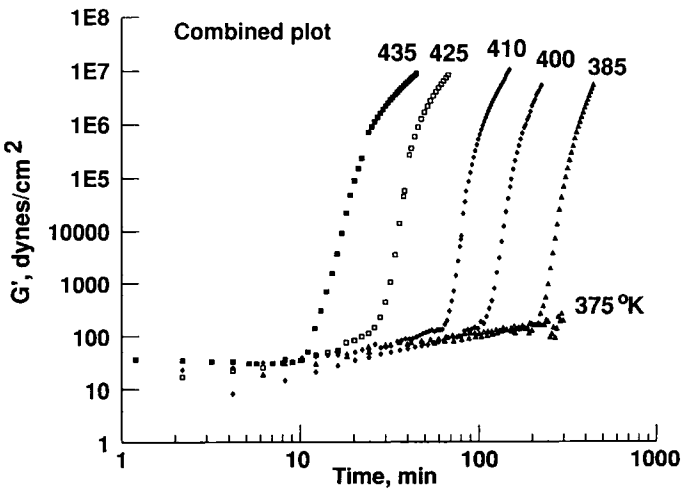

Fig. 7. Double logarithmic plots of $G'(t)$ for Hercules 3501-6 resin cured under six isothermal curing temperatures.

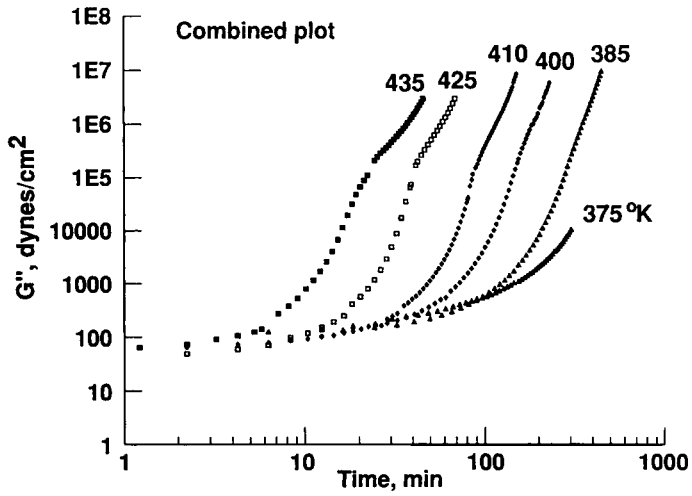

Fig. 8. Double logarithmic plots of $G''(t)$ for Hercules 3501-6 resin cured under six isothermal curing temperatures.

under various isothermal conditions have similar shapes. Attempts have been made to shift the curing curves both horizontally and vertically with respect to the curve of a selected reference cure temperature. The selected reference temperature was T_r = 400 K. A single master curve of (log G'') vs. (log t) obtained by this method is shown in Figure 9. The capability for data to be superimposed is generally satisfactory, except that the data at the two highest temperatures (425 and 435 K) consistently deviate from the main body of the master curve beyond the crossover points. The horizontal (reaction time) and vertical (modulus) shift factors $a_t(T)$ and $a_\eta(T)$, respectively, are defined by

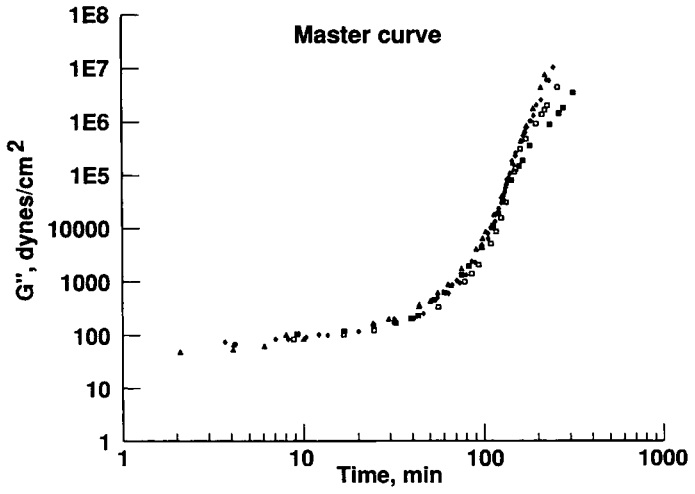

Fig. 9. Master curing curve of $G''(t)$ for Hercules 3501-6 resin cured under isothermal conditions.

TABLE VIII
Shift Factors $a_t(T)$ and $a_\eta(T)$ as Defined by Eqs. (6)and (7) for the Correspondence Effects of Curing Temperature and Time on the Hercules 3501-6 Resin System

T (K)	$1/T$ (10^{-3} K^{-1})	$a_t(T)$	$a_\eta(T)$
375	2.67	3.0	2.51
385	2.60	2.0	1.30
400	2.51	1.0	1.0
410	2.44	0.60	0.85
425	2.35	0.25	0.57
435	2.30	0.13	0.60

$$\log a_t(T) = \log t(T) - \log t(T_r) \tag{6}$$

and

$$\log a_\eta(T) = \log G''(T) - \log G''(T_r) \tag{7}$$

Values of $a_t(T)$ and $a_\eta(T)$ calculated from eqs. (6) and (7) are tabulated in Table VIII. The temperature dependency of the shift factors is plotted in Figure 10. Linear relationships are noted which suggest the adequacy of the following equations:

$$a_t(T) = A_t \exp(E_a/RT) \tag{8}$$

and

$$a_\eta(T) = A_\eta \exp(E_\eta/RT) \tag{9}$$

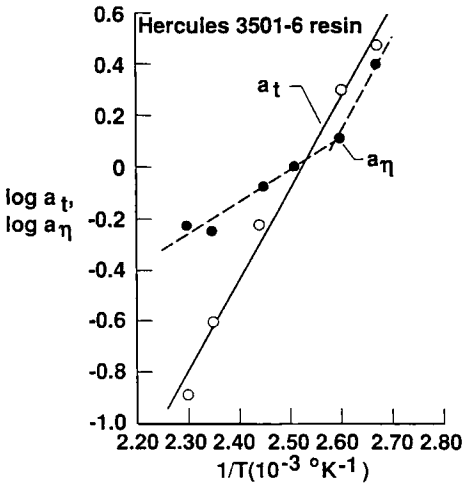

Fig. 10. Arrhenius plots of the shift factors $a_t(T)$ and $a_\eta(T)$.

to describe the relationship, where R is the ideal gas constant and T is the cure temperature in K. E_a and E_η denote the overall apparent activation energy of the polymerization reactions and the activation energy of viscous flow, respectively. An apparent change in slope of the log $a_\eta(T)$ vs. $(1/T)$ plot occurs near T = 385 K. By means of least squares fit to the data points in Figure 10, we have $E_a = E_\eta$ = 16.5 kcal/mol for $T \leq 385$ K and E_a = 16.5 kcal/mol, E_η = 5.60 kcal/mol for $T > 385$ K. The higher value of the apparent activation energy for the polymerization reaction for this particular resin system cured at temperatures above 385 K suggests that the chemical reaction mechanism is the overall rate limiting step for the advancement of the resin under isothermal curing conditions.

Applying the same shift factors $a_t(T)$ and $a_\eta(T)$ of the Table VIII to the storage modulus $G'(t)$, a single master curve can again be deduced as shown in Figure 11. This is expected since changes in both of the viscoelastic properties, $G'(t)$ and $G''(t)$, originate from the same reaction mechanism. The superposition of $G'(t)$ is, however, less satisfactory than that of $G''(t)$ in Figure 9.

Gelation Theory Applied to Epoxy Mixtures

It is of interest to compare the extent of reaction in the observed characteristic resin cure states with the predictions of reactions in a multifunctional reacting mixture. The theory[17] assumes that all groups react independently and that no intramolecular reactions occur in finite species.

There is some doubt about the exact composition of the resin used in the present study, but a typical formulation is given in Table I. Using the notation of Miller and Macosko,[17] this mixture has an effective epoxy functionality g_e of 3.88, an amine functionality f_e of 4.0, and an amine hydrogen:epoxy ratio r of 0.62. The predicted extent of reaction, p, at the gel point is obtained by solving

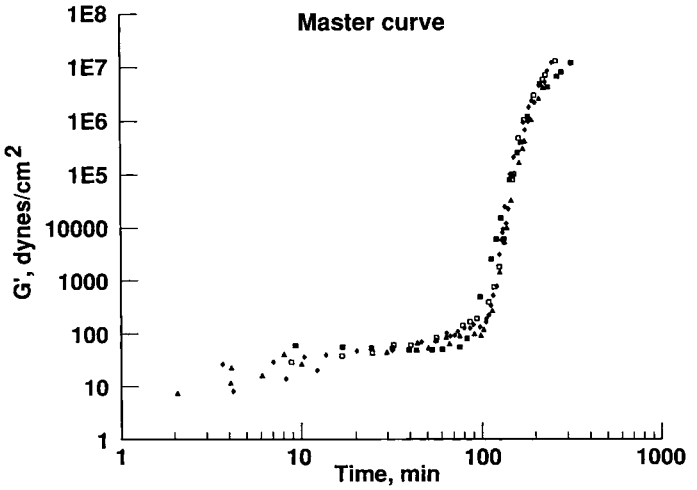

Fig. 11. Master curing curve of $G'(t)$ for Hercules 3501-6 resin system cured under isothermal conditions.

$$rp_{gel}^2 = 1/[(f_e - 1)(g_e - 1)]$$

This leads to $p_{gel} = 0.43$, i.e., at the gel point, 43% of the amine hydrogens and 27% of the epoxy groups have been used up.

The number-average molecular weight may always be calculated by dividing the total mass by the number of molecules present. Each bond formed decreases the number of molecules by one, so at the gel point, one calculates $M_n = 946$.

The above scheme is, of course, an idealization. At least three factors have been left out of the analysis. They are: (a) The major epoxy component is actually a commercial material, and not pure TGMDA; (b) the primary and secondary amine may have differing reactivities toward epoxy groups; (c) the BF_3 catalyst may promote homopolymerization of epoxy groups. Each of these factors will now be considered in turn.

(a) The "TGMDA" component comes in various viscosities[6,7] and may typically contain 20–30% by weight of dimers, trimers, and higher oligomers. The effect of oligomers on the gel point may be seen by considering, as an extreme example, a "TGMDA" consisting of 70% monomer and 30% trimer (assumed to have a functionality of 8). Then we obtain for the mixture $g_e = 4.60$, $r = 0.676$, and $p_{gel} = 0.37$, with $M_n = 970$. As expected, a mixture which contains epoxy oligomers gels more quickly.

(b) The possible substitution effect on amine reactivity is a matter of controversy. Charlesworth[18] found it to be negligible, whereas Dusek[19] claims it is significant, especially for DDS. The effect of reactivity ratio on gelation has been calculated by Bokare and Gandhi.[20] Results for some relevant cases are given in Table IX. Although a steric effect on amine reactivity delays gelation, the effect is not dramatic.

(c) Since the formulation contains a large excess of epoxide over amine hydrogen, there is little doubt that etherification (homopolymerization of epoxy

TABLE IX
Calculated Effects of Amine Reactivity and Epoxy Homopolymerization on Gel Point

		Gel point		
Relative amine rate constants, secondary : primary	Rate ratio 2° amine : epoxy + epoxy	Fraction of primary amine remaining (p/p_o)	Fractional conversion of epoxy groups ξ_e	Fractional conversion of amine hydrogens ξ_a
0.50	$\rightarrow\infty$ (no homopolymerization)	0.320	0.26	0.39
0.10		0.184	0.29	0.43
0.0002		0.093	0.31	0.46
0.50	1	0.428	0.24	0.32
0.10	1	0.24	0.28	0.40
0.0002	1	0.094	0.30	0.45
0.50	0.01	0.89	0.10	0.06
0.10	0.01	0.744	0.15	0.13
0.0002	0.01	0.12	0.30	0.44

groups) must occur, at least in the later stages of reaction. The importance of this mechanism is controversial[21] in uncatalyzed systems, but BF_3 complex is an efficient initiator of epoxy polymerization[22] as well as being (presumably) an accelerator for the epoxy/amine reaction.[6,7,23] The simultaneous occurrence of epoxy/amine addition and homopolymerization has again been treated by Bokare and Gandhi. Several special cases of the general results are tabulated in Table IX. Note that there is an error in eq. (A5) of Ref. 21; this has been corrected. From these results it appears that, for any reasonable combination of kinetic parameters, the gel point should occur below 30% conversion of epoxy groups. The rheological measurements, on the other hand, indicate little crosslinking up to $\alpha_o \cong 0.6$. Thus either the determination of α is in error, or the assumptions of the gelation theory are not fulfilled in this system.

In fact, there is reason to question the DSC measurement of extent of reaction, since it was based on the assumption that α is proportional to the cumulative heat of reaction. Due to the difference between the primary amine–epoxy reaction and the other curing reactions, this assumption leads to overestimates of the reaction rate.[24,25] A sample calculation using the data in Ref. 25 shows that the error in α should be only about 10% near $\alpha = 0.6$, however.

Therefore, we tentatively conclude that the gelation theory does not apply to this commercial system. A likely reason is that the crosslinking is not as homogeneous as the theory assumes. Given the difficulty of dispersing the solid diamine in a viscous resin, this would not be too surprising. An independent verification of the gel time from steady shearing or solubility measurement would be of interest, however. It is possible that storage or batch-to-batch variations might have affected the concentration of catalyst.

CONCLUSIONS

Measurements of the changes of rheological properties of the Hercules 3501-6 resin system cured under six isothermal conditions between 375 and 435 K were made on a Rheometrics System 4 rheometer. The changes in storage modulus $G'(t)$ and loss modulus $G''(t)$ curing curves were followed by small amplitude oscillatory dynamic experiments using a parallel-plate configuration.

Two characteristic material states were identified: the gelation point manifests itself by an abrupt change in slope of the $G'(t)$ curve at curing temperatures of 385 K and above and a crossover point between the $G'(t)$ and $G''(t)$ curves was observed at curing temperatures of 400 K and above. In each characteristic material state, the same degree of cure was reached for resin samples cured isothermally at different temperatures. The temperature dependence of viscosity in each of these two characteristic material states was shown to follow the Arrhenius type relationship, which suggested that the glass transition temperature T_g remains constantly less than $(T_d - 100)$ K up to the crossover point during curing at temperature T_d. Such behavior had also been observed by DSC thermal analysis conducted on the same resin system. By comparing the activation energy of the polymerization reaction and that for viscous flow in each characteristic material state, it was revealed that within the range of curing temperatures investigated here, the mechanism of chemical reaction was the rate limiting step for the advancement of the resin system at the gelation point, whereas, at the crossover point, the limiting step became diffusion controlled.

It was found that the curing behavior of the Hercules 3501-6 resin system at various temperatures can be unified by the technique of time-temperature superposition. The temperature dependent shift factors for moduli and reaction times indicated that at $T \geq 385$ K, the polymerization reaction kinetics was the limiting step for overall advancement of the reactive resin system. At curing temperatures below 385 K, however, the diffusion mechanism and the reaction kinetics played equal roles. The method of rheological analysis discussed here should be useful in the processing of commercially interesting thermosetting materials.

An attempt to calculate the extent of reaction at the gel point using the expectation theory of Miller and Macosco gave results in serious disagreement with the experimental determination. The latter, however, depends on DSC measurements from another laboratory published 7 years ago. It is suggested that lack of homogeneity in the material may account for the discrepancy.

References

1. R. P. White Jr., *Polym. Eng. Sci.*, **14**, 50–57 (1974).
2. F. G. Mussatti and C. W. Macosko, *Polym. Eng. Sci.*, **13**, 236–240 (1973).
3. A. Apicella, P. Masi, and L. Nicolais, *Rheol. Acta*, **23**, 291 (1984).
4. J. M. Castro, C. W. Macosko, and S. J. Perry, *Polym. Commun.*, **25**, 82 (1984).
5. T. A. Sewell, "Chemical Composition and Processing Specifications for Air Force/Navy Advanced Composite Matrix Materials," F33615-78-C-5177, McDonnell Aircraft Co., St. Louis, MO, 1982.
6. R. J. Morgan, C. M. Walkup, and T. H. Hoheisel, *J. Compos. Technol. Res.*, **7**(1), (1985).
7. J. F. Carpenter, "Processing Science for AS/3501-6 Carbon/Epoxy Composites," McDonnell Aircraft Company Technical Report No. 19-81-C-0184, 1983.
8. W. I. Lee, A. C. Loos, and G. S. Springer, *J. Comps. Mater.*, **16**, 510–520 (1982).
9. D. Stauffer, A. Coniglio, and M. Adam, *Adv. Polym. Sci.*, **44**, 74 (1982).
10. C. Y. M. Tung and P. J. Dynes, *J. Appl. Polym. Sci.*, **27**, 569 (1982).
11. H. H. Winter, *Polym. Eng. Sci.*, **27**(22), 1698–1702 (1987).
12. H. H. Winter and F. Chambon, *J. Rheol.*, **30**(2), 367–382 (1986).
13. W. P. Cox and E. H. Merz, *J. Polym. Sci.*, **28**, 619 (1958).
14. R. B. Bird, R. C. Armstrong, and O. Hassager, *Dynamics of Polymeric Liquids*, Wiley, New York, 1977.
15. J. D. Ferry, *Viscoelastic Properties of Polymers*, 3rd ed., Wiley, New York, 1980.
16. T. H. Hou and J. M. Bai, *SAMPE J.*, **24**, 43–51 (1988).
17. D. R. Miller and C. W. Macosko, *Macromolecules*, **9**(2), 206 (1976).
18. J. Charlesworth, *J. Polym. Sci. Polym. Chem. Ed.*, **18**, 621 (1980).
19. K. Dusek, *Am. Chem. Soc. Org. Coat. Prepr.*, **49**, 378 (1983).
20. U. M. Bokare and K. S. Gandhi, *J. Polym. Sci. Polym. Chem. Ed.*, **18**, 857 (1980).
21. J. M. Charlesworth, *J. Polym. Sci. Polym. Phys. Ed.*, **17**, 1557 (1979).
22. J. J. Harris and S. C. Temin, *J. Appl. Polym. Sci.*, **10**, 523 (1966).
23. C. A. May, M. R. Dusi, et al., *Am. Chem. Soc. Org. Coat Prepr.*, **47**, 419 (1982).
24. A. Gupta, M. Cizmecioglu, D. Coulter, R. H. Liang, A. Yavrouian, F. D. Tsay, and J. Moacanin, *J. Appl. Polym. Sci.*, **28**, 1011 (1983).
25. A. Apicella, L. Nicolais, M. Iannone, and P. Passerini, *J. Appl. Polym. Sci.*, **29**, 2083 (1984).

Received September 5, 1989
Accepted November 6, 1989